Electronic Supplementary Material (ESI) for Inorganic Chemistry Frontiers.

Supporting Information

Selective and Rapid Detection of Ascorbic Acid by Cobalt Oxyhydroxide-Based Two-Photon Fluorescent Nano-Platform

Qingxin Han[a], Huan Yang[a], Shuting Wen[b], Huie jiang[a, c], Li Wang[a], and Weisheng Liu[a]*

[a] *State Key Laboratory of Applied Organic Chemistry, Key Laboratory of Nonferrous Metal Chemistry and Resources Utilization of Gansu Province, College of Chemistry and Chemical Engineering, Lanzhou University, Lanzhou 730000, China.*

[b] *Lanzhou University Second Hospital, Lanzhou 730000, China.*

[c] *College of Bioresources Chemistry and Materials Engineering, Shaanxi University of Science and Technology, Xi'an 710021, China.*

* *Corresponding author. Tel: +86/931/8915151*

Fax number: +86/931/8912582

E/mail: liuws@lzu.edu.cn

Table of Contents

Table S1. Comparison of CoOOH based fluorescent probes for AA.

Probe	Easy preparation or not	NIR excitation or not	Linear range (μM)	Detection limit (μM)	Quantum yield	Reference
CoOOH-modified PLNPs	Not	Not	1-100	0.59	Low	Ref. 11
Tris-derived CDs-CoOOH	Not	Not	0.1-20	0.05	High	Ref. 12
CoOOH-modified UCNPs	Not	NIR	0-60	0.20	Low	Ref. 13a
Silica nanoparticles	Not	NIR	1-20	0.17	moderate	Ref. 13b
Graphene quantum dots	Not	NIR	1-30	0.27	moderate	Ref. 13c
Our ratiometric nanoprobe	Not	NIR	1-50	0.63	Low	Ref. 14
MBNI-CoOOH nanosheets	Easy preparation	NIR	0-100	0.26	High	This work

Supporting Figures:

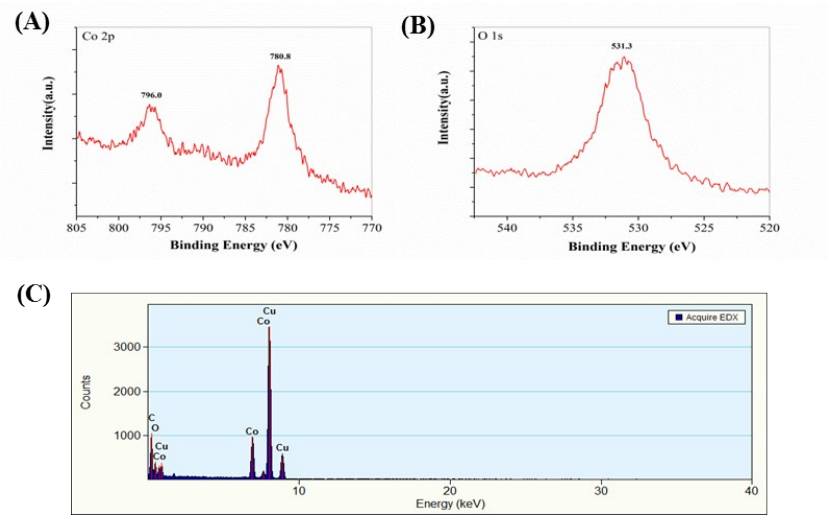

Fig. S1. (A) XPS spectrum of Co 2p from the CoOOH nanosheets. (B) XPS spectrum of O 1s from the CoOOH nanosheets. (C) EDX spectrum of the CoOOH nanosheets.

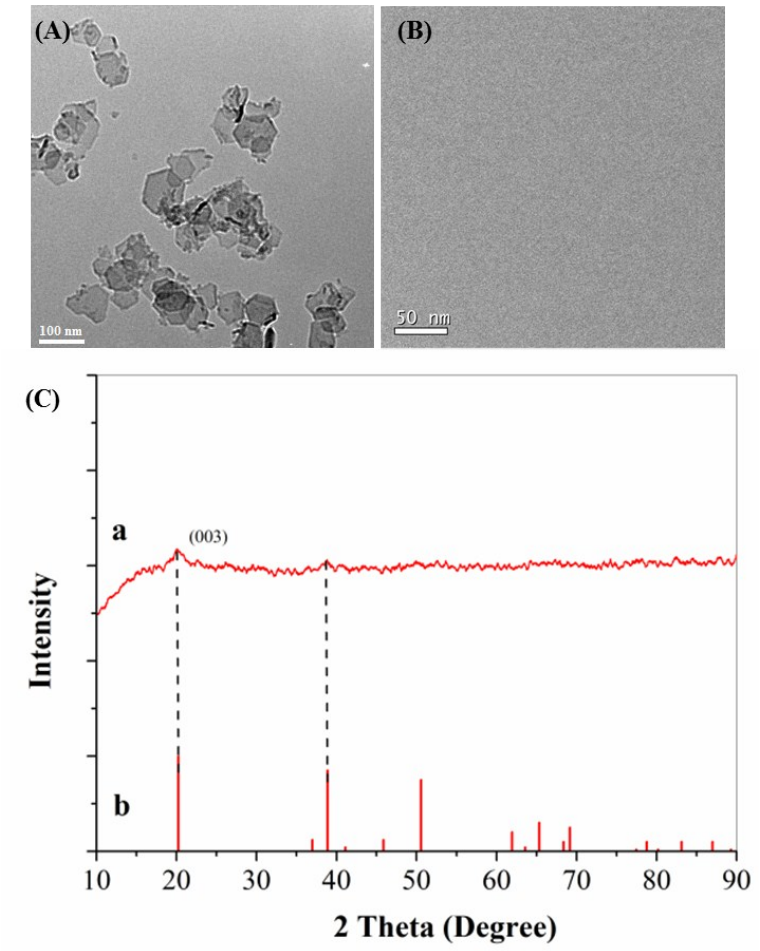

Fig. S2. (A) TEM image of the CoOOH-based nano-platform. (B) TEM image of the CoOOH-based nano-platform after reacted with AA. (C) XRD pattern of the as prepared CoOOH nanosheets (a) and standard XRD patterns for CoOOH nanocrystals (JCPDS, Card No.07-0169).

These characterization results demonstrated the formation of CoOOH nanosheets. When the nano-platform was treated with AA, the CoOOH nanosheets disappeared from TEM image (**Fig. S2B**). Nevertheless, no obvious diffraction peaks corresponding to the hexagonal CoOOH nanosheets were observed in X-ray diffraction (XRD) pattern (**Fig. S2C**), indicating the prepared CoOOH nanosheets was mainly amorphous phase.

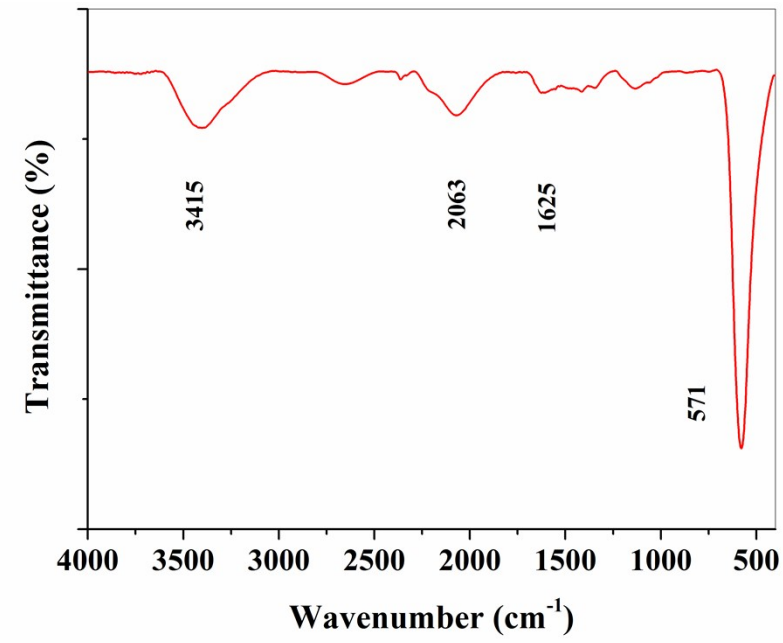

Fig. S3. (A) FT-IR spectrum of CoOOH nanosheets.

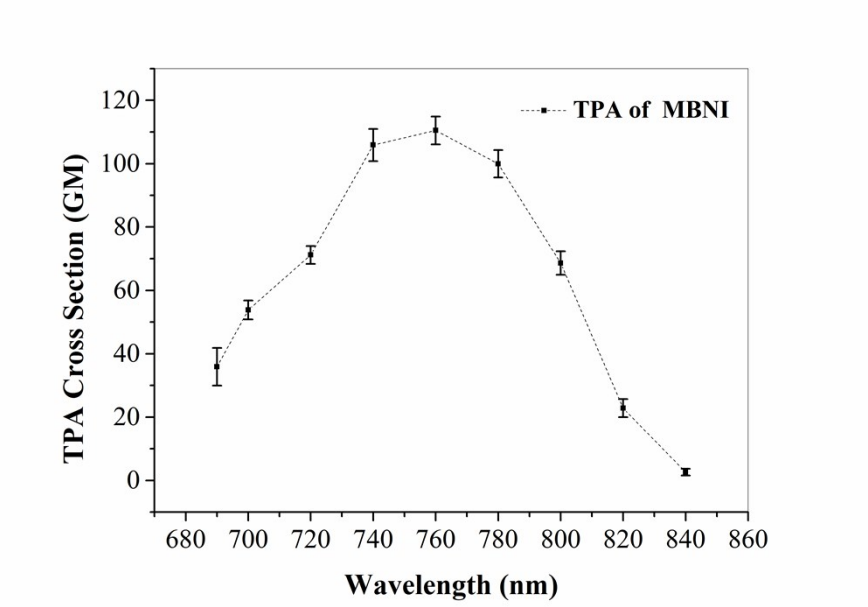

Fig. S4. TPA cross section of MBNI in HEPES buffer solution (10 mM, pH 7.40, containing 0.5% DMSO).

Since it is usually only a small fraction of photons is absorbed by two-photon (TP) dyes in the TP process, TP fluorescence excitation is an alternative approach to determining TP fluorescence excitation (TPE) cross sections, provided that the dye is fluorescent and that its fluorescent quantum efficiency is known. In this study, the TPA cross section (δ) for **MBNI** were determined in HEPES buffer solutions (10 mM, pH 7.40, containing 0.5% DMSO). The TPA cross section:

$$\delta_M = \frac{\delta_{ref} \times A_M \times \Phi_{ref} \times \varphi_{ref} \times c_{ref}}{A_{ref} \times \Phi_M \times \varphi_M \times c_M}$$

Where the subscripts *M* stand for the TP dye (MBNI) and ref is the reference molecules, fluorescein (2.5 μM, pH = 13.0). *A* is integral of fluorescence intensity that collected by a CCD detector. The fluorescence quantum yield was denoted as Φ. *c* is the mole concentration. The overall fluorescence collection efficiency of the experimental apparatus was denoted as φ.

The absolute quantum yield Φ of MBNI in HEPES buffer solution (10 mM, pH 7.40, containing 0.5% DMSO) was determined by an absolute method using an integrating sphere (150 mm diameter, $BaSO_4$ coating) on Edinburgh Instrument FLS920, and by using the following equation:

$$QY = \frac{\varepsilon}{\alpha} = \frac{L_S}{E_b - E_S}$$

Where $\boldsymbol{QY}$ is the quantum yield, $\boldsymbol{\varepsilon}$ is the number of photons emitted by the sample, $\boldsymbol{\alpha}$ is the number of photons absorbed by the sample; $\boldsymbol{L_s}$ is the fluorescence spectrum of the sample, collected using integrating sphere; $\boldsymbol{E_b}$ is the spectrum of the light in the absence of sample in the sphere, collected using integrating sphere; $\boldsymbol{E_s}$ is the spectrum of the light used to excite the sample, collected using the integrating sphere. The sample was measured three times and the final value of quantum yield corresponds to the arithmetic mean value.

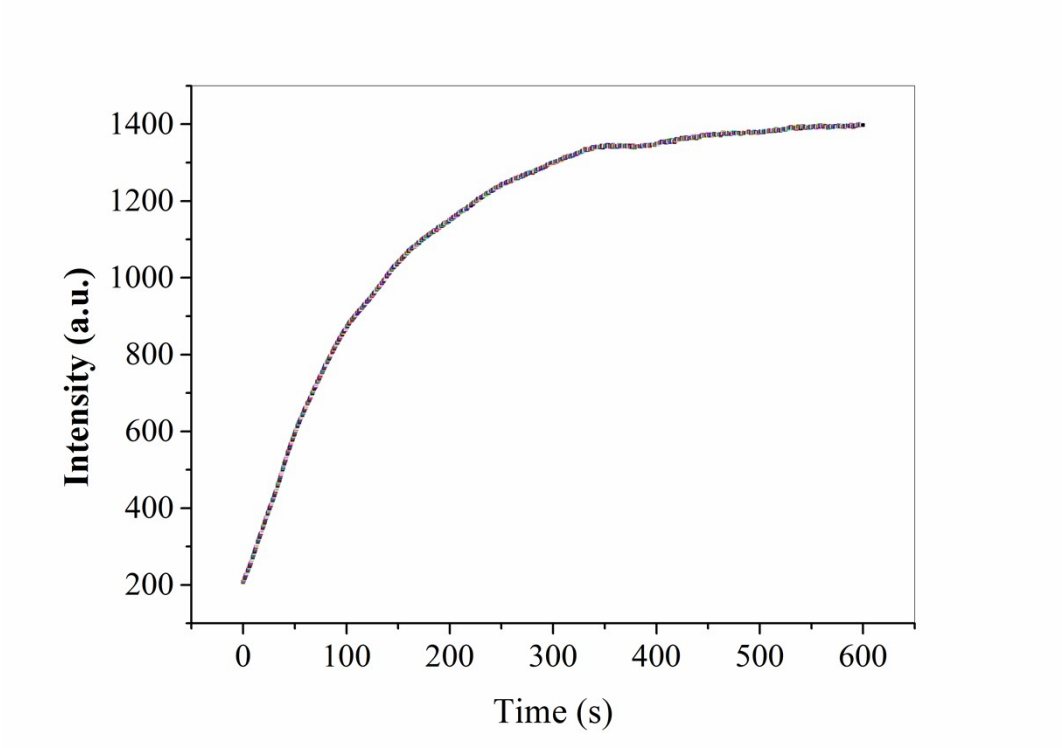

Fig. S5. Real-time records for fluorescence intensity (λ_{ex}= 750 nm, λ_{em}= 470 nm) changes of CoOOH-based nano-platform in the presence of AA (200 μM).

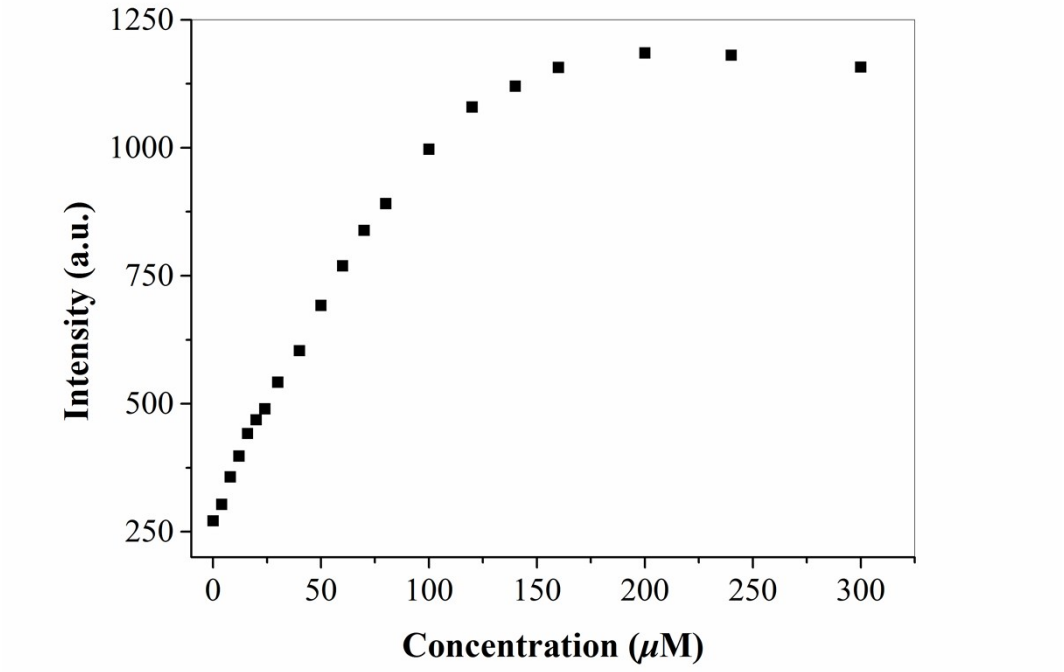

Fig. S6. The fluorescence intensity (λ_{ex}= 750 nm, λ_{em}= 470 nm) of CoOOH-based nano-platform versus varied concentrations of AA, the fluorescence intensity of each point was record at 5min.

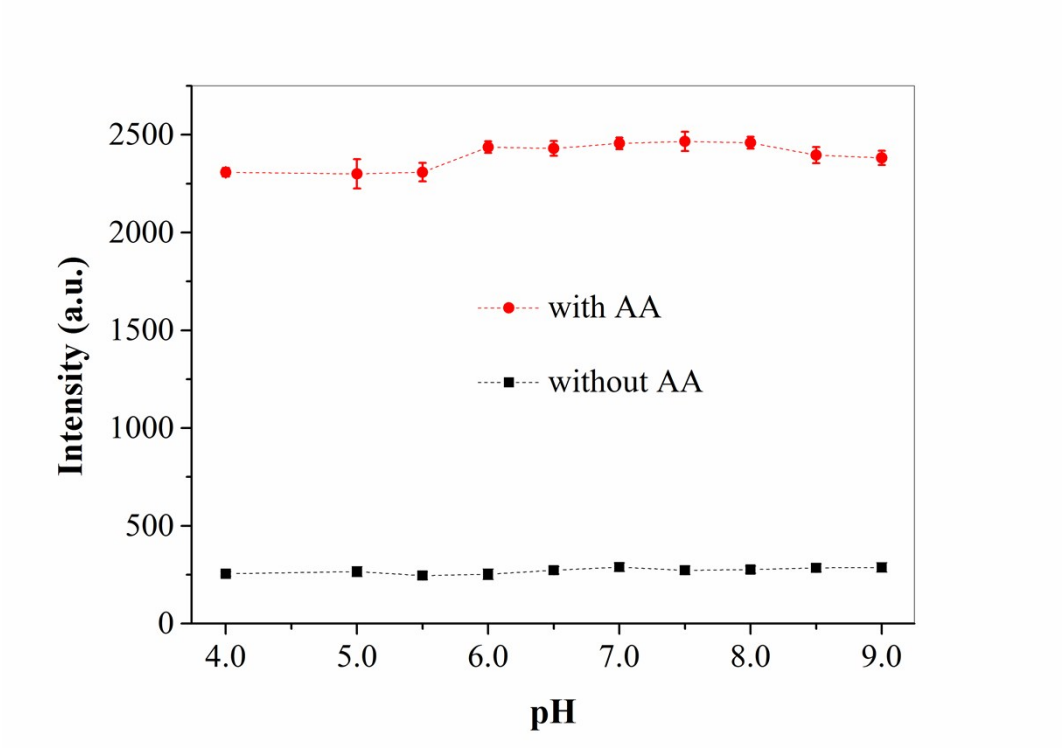

Fig. S7. The effects of pH values on the fluorescence intensity (λ_{ex}= 750 nm, λ_{em}= 470 nm) of CoOOH-based nano-platform in the absence (black dots) and presence (red dots) of AA (200 μM).

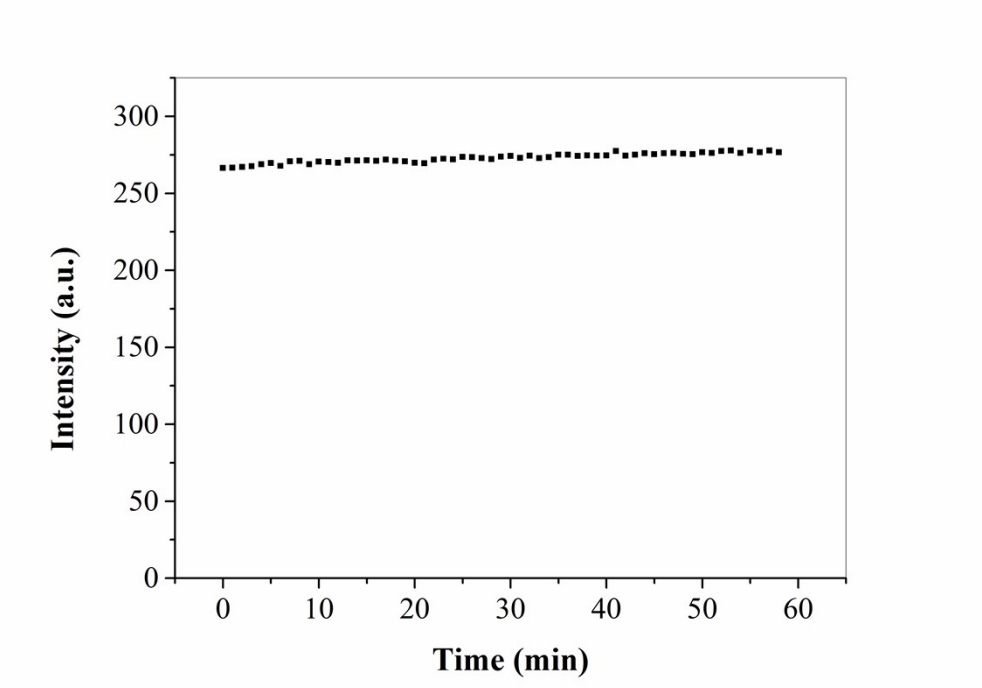

Fig. S8. Time-dependent fluorescence intensity (λ_{ex}= 750 nm, λ_{em}= 470 nm) changes of CoOOH-based nano-platform in HEPES buffer solution (10 mM, pH 7.40, containing 0.5% DMSO).

This result demonstrates that the dye-CoOOH hybrid nanosheets could keep stable in HEPES

buffer solution at least for an hour, which is long enough for AA detection.

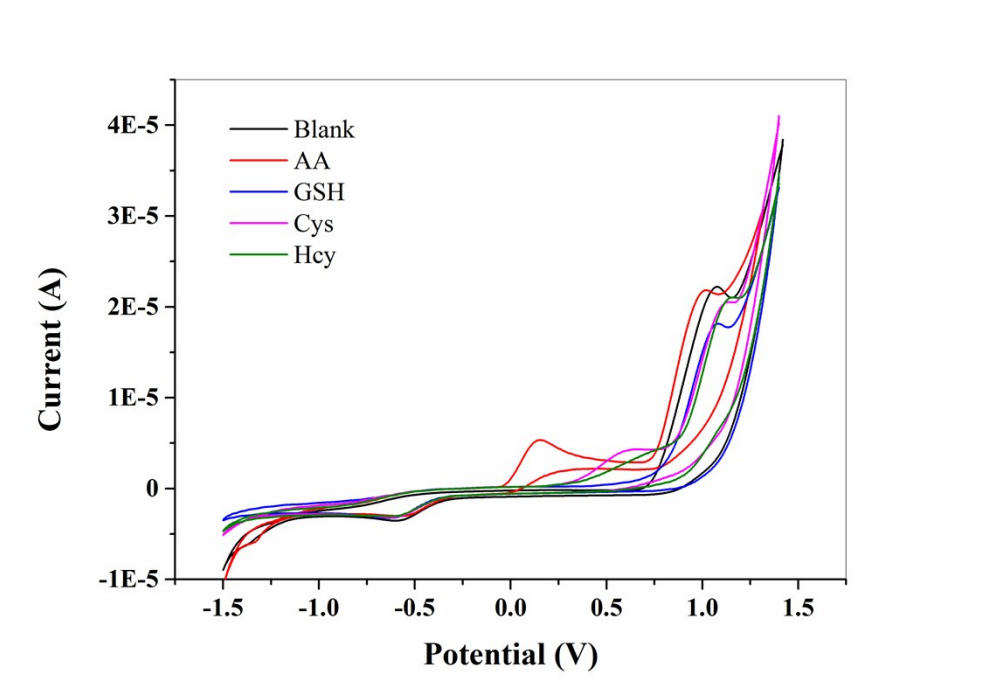

Fig. S9. Cyclic voltammograms of 1mM AA, GSH, Cys and Hcy in HEPES solution (10 mM, pH = 7.40).

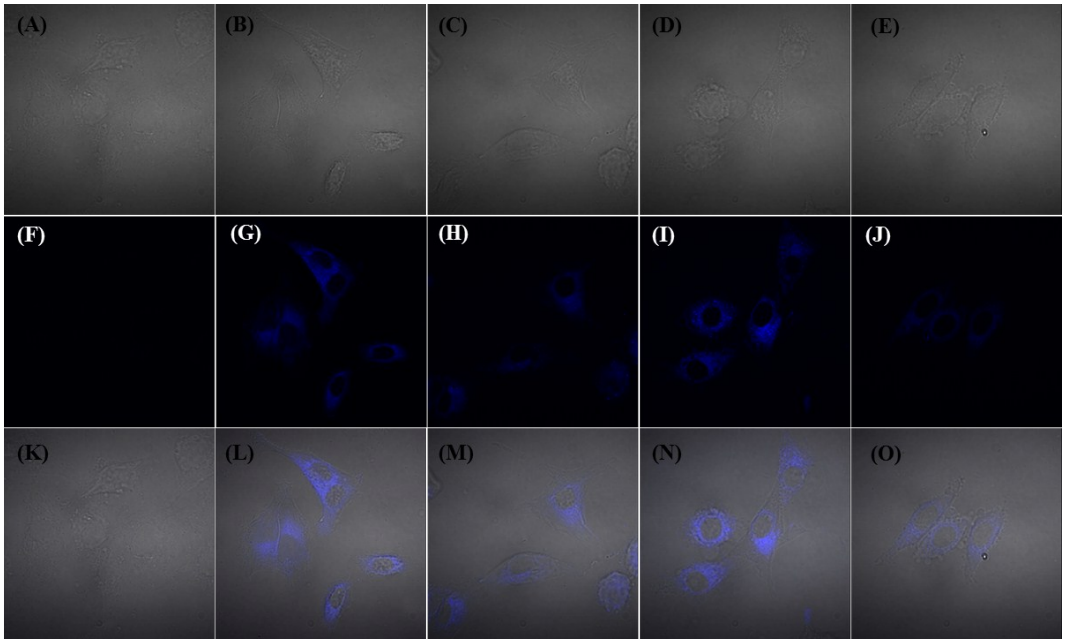

Fig. S10. TP fluorescence images in living HeLa cells. (A, F, K) HeLa cells were incubated with CoOOH nanosheets (0.1 mM) for 15 min. (B, G, L) HeLa cells were incubated with MBNI (5 μM) for 15 min at 37 °C. (C, H, M) HeLa cells were incubated with MBNI (5 μM) for 15 min and further incubated with CoOOH nanosheets (0.1 mM) for another 15 min. (D, I, N) HeLa cells were successively incubated with MBNI (5 μM), CoOOH nanosheets (0.5 mM), and AA (250 μM) for 15

min. (E, J, O) HeLa cells were pretreated with 10 U/μL AOase (10 U/μL) for 1.0 h, and then successively incubated with MBNI (5 μM), CoOOH nanosheets (0.5 mM). (A-E) are the bright-field images corresponding to (F-J), respectively. (K-O) are the overlay images.

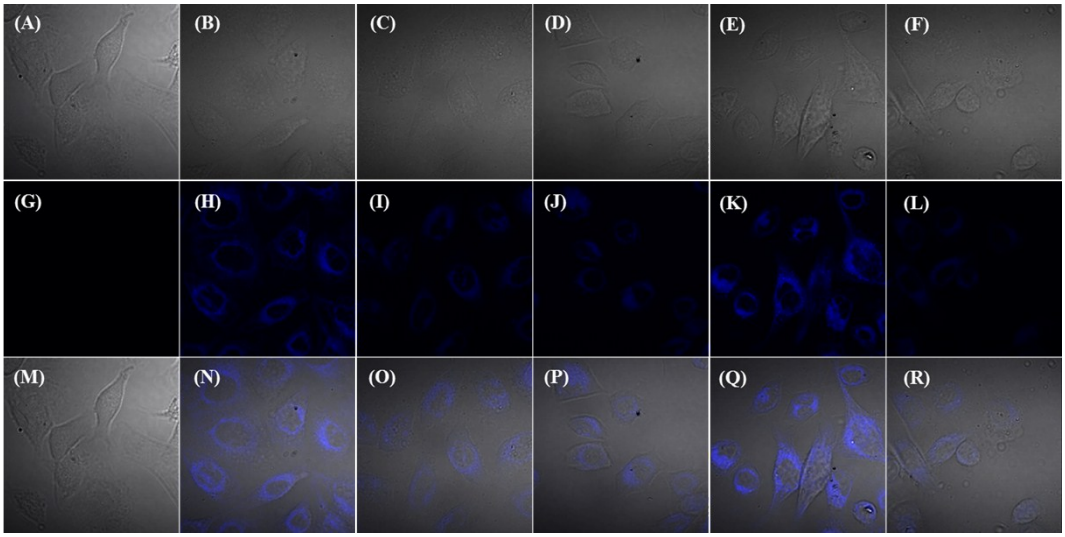

Fig. S11. TP fluorescence images in living AGS cells. (A, G, M) AGS cells were incubated with CoOOH nanosheets (0.1 mM) for 15 min. (B, H, N) AGS cells were incubated with MBNI (5 μM) for 15 min at 37 °C. (C, I, O) AGS cells were incubated with MBNI (5 μM) for 15 min and further incubated with CoOOH nanosheets (0.1 mM) for another 15 min. (D, J, P) AGS cells were incubated with CoOOH nanosheets (0.1 mM) for 15 min and further incubated with MBNI (5 μM) for another 15 min. (E, K, Q) AGS cells were successively incubated with MBNI (5 μM), CoOOH nanosheets (0.5 mM), and AA (250 μM) for 15 min. (F, L, R) AGS cells were pretreated with 10 U/μL AOase (10 U/μL) for 1.0 h, and then successively incubated with MBNI (5 μM), CoOOH nanosheets (0.5 mM). (A-F) are the bright-field images corresponding to (G-L), respectively. (M-R) are the overlay images.

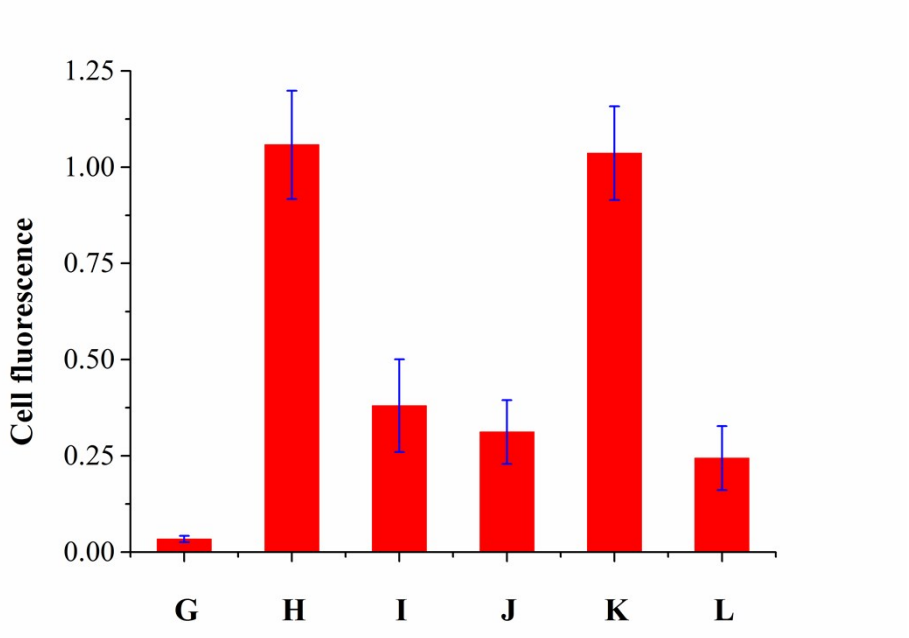

Fig. S12. Cells fluorescence corresponding to **Fig. S11** (G-L)**.** The intensities of cell were measured by FIJI-ImageJ software which is an open-source platform for biological-image analysis (http://imagej.net/Fiji)[1]. The following equation was used to correct measured fluorescence intensities: IntDen (corrected) = IntDen-Area*Mean (background).

As shown in **Fig S12**, compared with un-pretreated AGS cells, the fluorescence of the AGS cells pretreated with AOase[2] reduced when further incubated with CoOOH-based nano-platform, indicating that CoOOH-based nano-platform is potentially to determine intracellular AA detection.

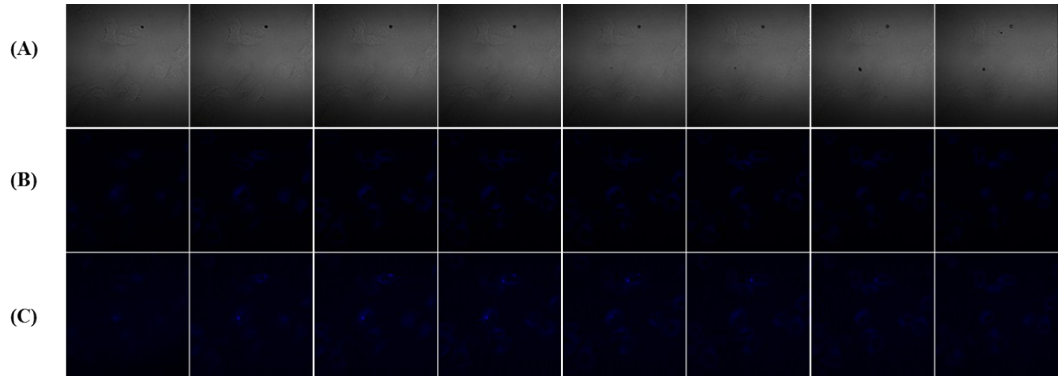

Fig. S13. Z-scan confocal images of the living AGS cells incubated with CoOOH-based nano-platform. (A) Bright field imaging. (B) TP fluorescence imaging with excitation of 750 nm. (C) OP fluorescence imaging with excitation of 405 nm.

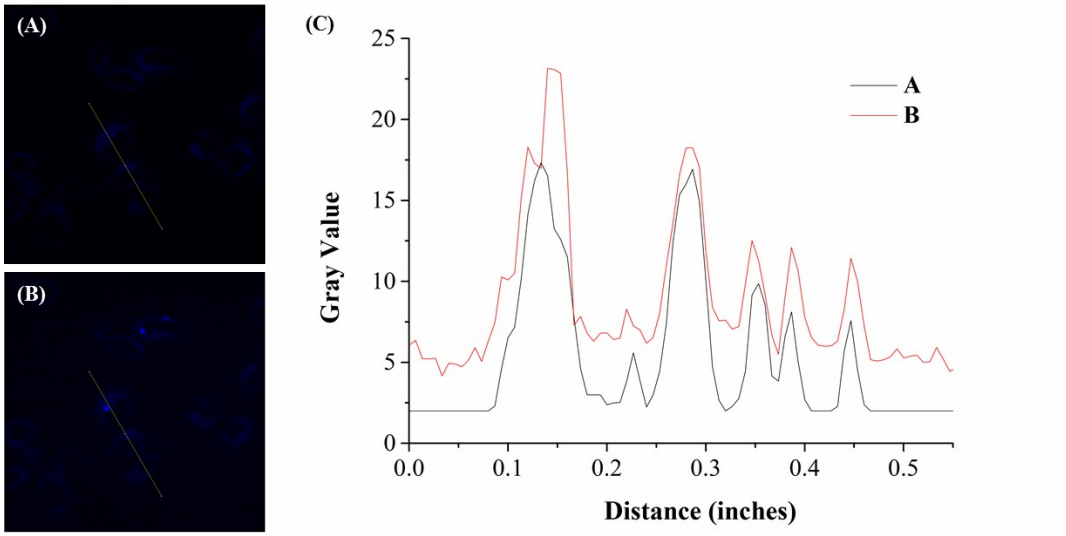

Fig. S14. Median section of Z-scan confocal images from **Fig. S13**. (A) TP fluorescence imaging. (B) OP fluorescence imaging. (C) Plot profiles corresponding to the yellow line in (A, black) and (B, red). Images were firstly converted into 8-bit grayscale and then measured by FIJI-ImageJ software.

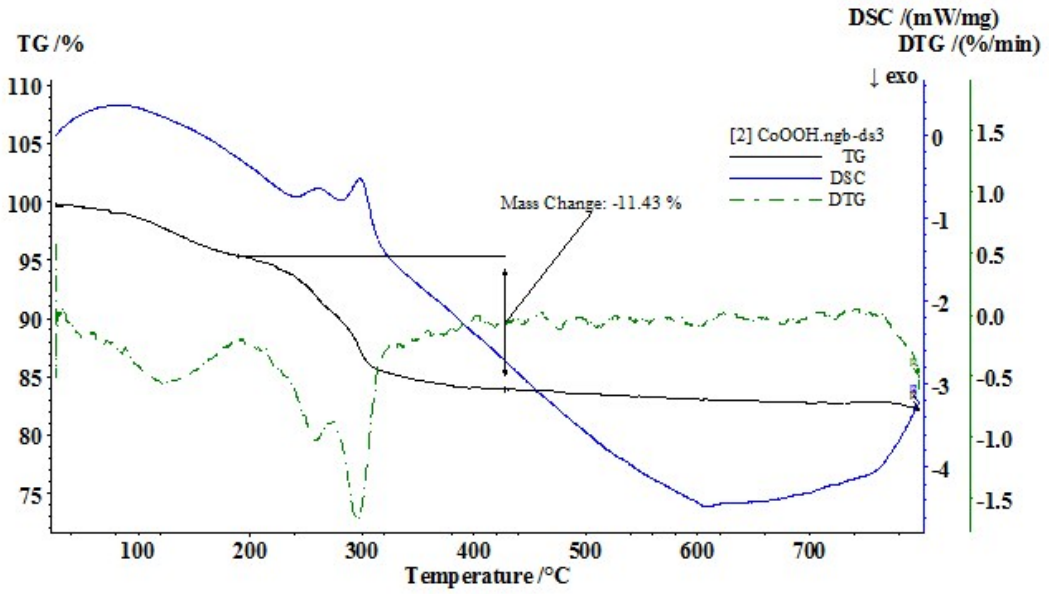

Fig. S15. TG-DSC result of CoOOH nanosheets.

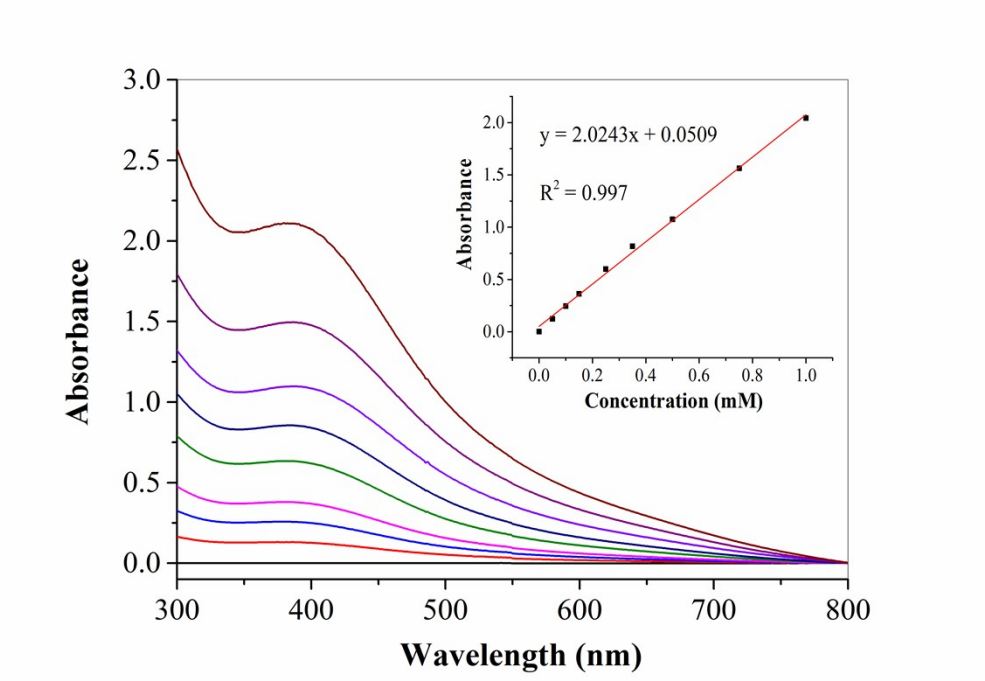

Fig. S16. Absorption spectra of CoOOH of different concentration (0.00, 0.05, 0.10, 0.15, 0.25, 0.35, 0.50, 0.75, 0.10 mM). Insert: the linear changes of absorbance at 405 nm versus the concentration of CoOOH in water solutions at room temperature.

Determination of CoOOH concentration:

Since the reaction that Co(II) oxidizes into CoOOH with ClO^- in alkali aqueous solution is very efficient, different concentrations (0.00, 0.05, 0.10, 0.15, 0.25, 0.35, 0.50, 0.75, 0.10 mM) of $CoCl_2$ were used to prepare CoOOH in-situ in the presence of excess ClO^- (2 mM) and OH^- (8 mM). Thus, the reaction was supposed to be 100% completion and the UV-vis spectrum of each concentration was recorded. As shown in **Fig. S16**, a well-fitting function between the concentration of CoOOH and the absorbance at 405 nm was obtained. This linear function (y = 2.0243x + 0.0509) could be used to determine the concentration of CoOOH. Then, ICP-AES experiment was conducted to investigate whether COHN can be reduced by GSH in living cells. ICP-AES experiments were conducted to investigate whether the concentration of CoOOH determined by UV spectrophotometry was reasonable. The result shows that the concentration of CoOOH determined by UV spectrophotometry (0.100 mM) was consistent with that determined by ICP-AES assay (0.104 mM). Thus, we have employed UV spectrophotometry and the linear function to determine the concentration of CoOOH in our study.

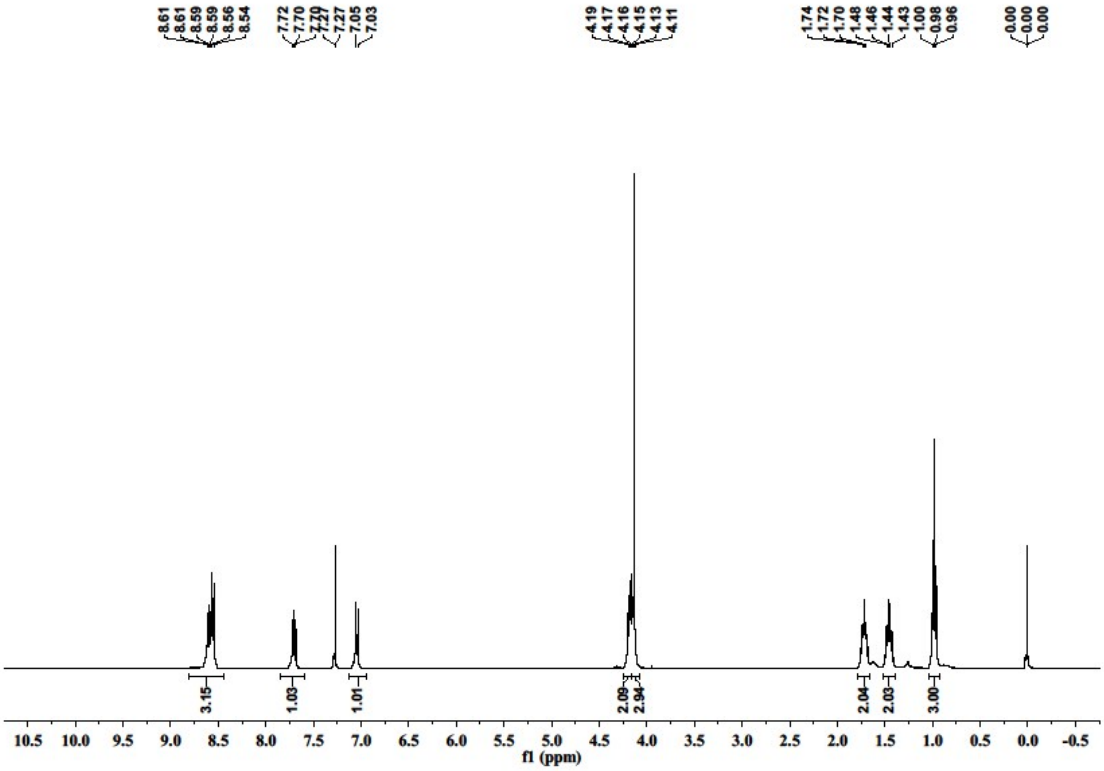

Fig. S17. ^{1}H NMR (400 MHz) spectrum of MBNI in $CDCl_3$.

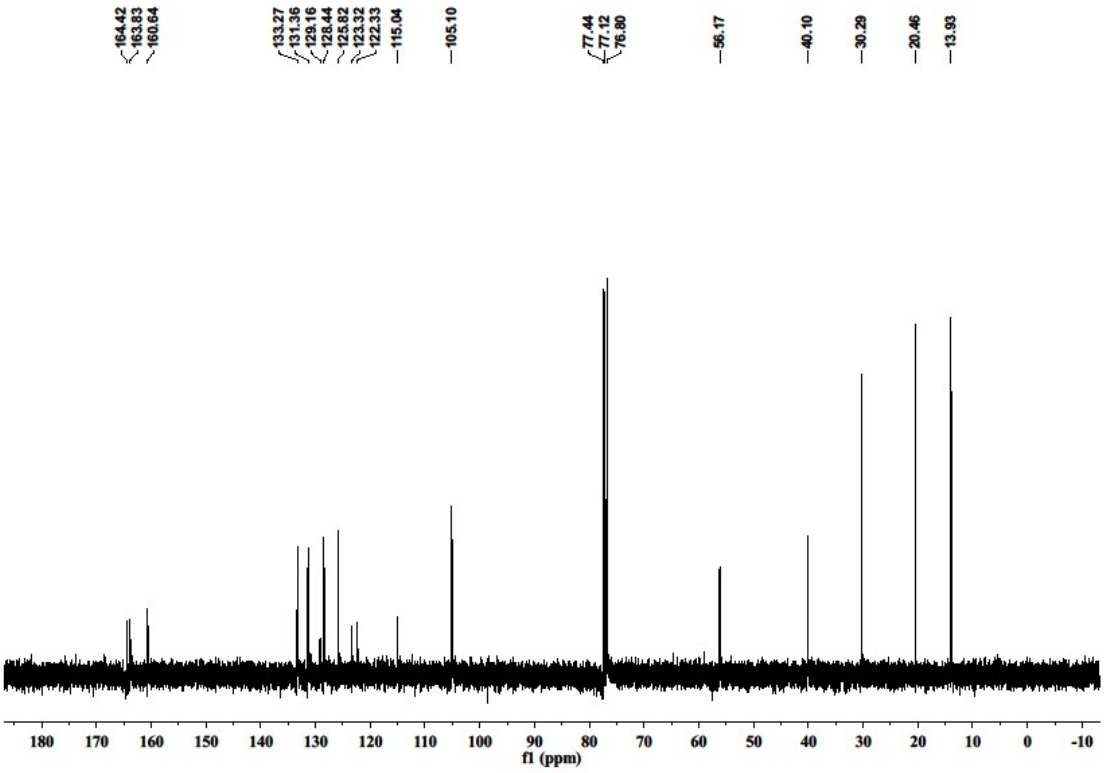

Fig. S18. ^{13}C NMR (101 MHz) spectrum of MBNI in $CDCl_3$.

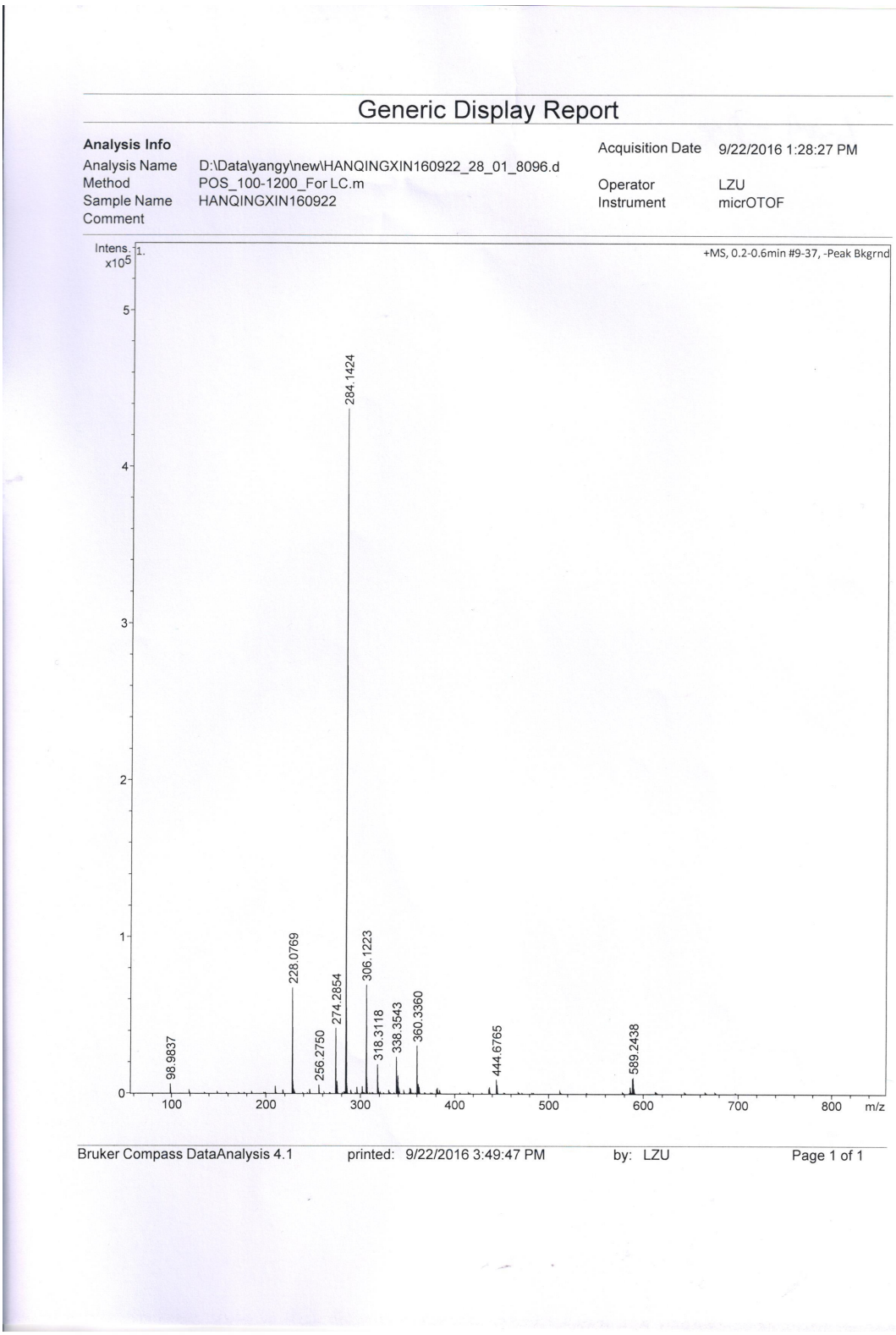

Fig. S19. Mass spectrum (ESI) of MBNI in $CDCl_3$.

References

[1] Schindelin, Johannes, et al. "Fiji: an open-source platform for biological-image analysis." Nature methods, 2012, 9 (7): 676-682.

[2] Feng, Li-Li, et al. "Near infrared graphene quantum dots-based two-photon nanoprobe for direct bioimaging of endogenous ascorbic acid in living cells." Analytical Chemistry, 2017, 89 (7): 4077-4084.

[3] De Mello, John C., H. Felix Wittmann, and Richard H. Friend. "An improved experimental determination of external photoluminescence quantum efficiency." Advanced materials, 1997, 9 (3): 230-232.